

## Journal of Material Sciences and Engineering Technology

# Experimental and Numerical Studies of Interlaminar Shear Strength in Basalt Fiber Reinforced Polymer Matrix Composite

Shubham Kavitkar, Singh KK and Hemant Priyadarshi

Department of Mechanical Engineering, IIT (ISM), Dhanbad 826004, Jharkhand, India

### \*Corresponding author

Shubham Kavitkar, Department of Mechanical Engineering, IIT (ISM), Dhanbad 826004, Jharkhand, India

Received: July 15, 2025; Accepted: July 25, 2025; Published: August 04, 2025

### ABSTRACT

Basalt fiber-reinforced polymer (BFRP) is a natural composite derived from volcanic rock through melting and fiberizing process. It is gaining popularity because of its high strength-to-weight factor and excellent mechanical, thermal and chemical properties. Fracture toughness testing is used to analyse crashworthiness, structural integrity and safety to avoid material failure. In this study, the estimation of Interlaminar Shear Strength (ILSS) was done by performing the Short Beam Shear (SBS) test. This three-point bend test is performed in accordance with the ASTM D2344 standard on a computerized Universal Testing Machine (UTM). Strain rate of 1 mm/min is given to the load cell. For this standard, the sample dimensions used are 36 x 12 x 6 mm<sup>3</sup>. The stacking sequence used in this study is [(0/90), (45/-45), (0/90), (45/-45)]<sub>2s</sub>. This test provides critical data on shear failure between the layers. The study compares the obtained experimental results with the numerical results from ANSYS. These results indicate excellent resistance to crack propagation and better interlaminar shear resistance. Matrix cracking, fiber breakage, crack initiation, delamination, debonding etc. such failure mechanisms are expected to occur.

**Keywords:** BFRP, ILSS, Delamination, ANSYS

### Introduction

Basalt fiber is a natural material derived from the fine fibers of volcanic rock that forms from rapid cooling of lava. They are known for their high factor of strength-to-weight, durability, resistance to corrosion and high temperature. Santosh Kumar examined the temperature effect on ILSS behaviour of basalt fiber [1]. The loading was done inside a closed furnace at room temperature, 50°C and 80°C. The decrease in shear strength was found as the temperature was increased. Similar results were obtained by W.J. Huang [2]. They conducted an experiment to examine how high and cryogenic temperatures affect the interlaminar shear strength (ILSS) behaviour of Carbon fiber composites. P Rama Lakshmi determined the distribution of ILSS in neat glass epoxy composites [3]. In this study, thin (thickness 2mm) and thick (thickness 10mm) plates were used according to ASTM D2344 and ASTM C1425 respectively. And

then the experimental results were validated by the finite element method. Chandan Kumar determined the ILSS of carbon/epoxy laminates which were highly doped with MWCNTs at different loading rates [4]. It was found that the ILSS values were increased by increasing strain rate, but up to a certain limit; after that it was decreased. ILSS value peaked at 3% doping of MWCNT. Nisha Sharma examined the flexural and fatigue behaviour of symmetric and asymmetric GFRP [5]. Flexural strength was found higher in case of symmetric than asymmetric laminate. It was concluded that at 0.5 stress level damage was concentrated and uniform but at 0.9 stress level it was severe and delocalised.

Aying Zhang studied the mechanical properties of carbon/epoxy composites having different void fractions [6]. There was a significant decrease in bending and compressive strength, interlaminar strength with an increase in void content. This was also compared with the finite element simulations done using ABAQUS. Pallela Rama Lakshmi did a finite element analysis

**Citation:** Shubham Kavitkar, Singh KK, Hemant Priyadarshi. Experimental and Numerical Studies of Interlaminar Shear Strength in Basalt Fiber Reinforced Polymer Matrix Composite. *J Mat Sci Eng Technol*. 2025. 3(3): 1-5. DOI: doi.org/10.61440/JMSET.2025.v3.61

on neat and CNT reinforced S-glass composites to estimate ILSS values [7]. There was a decrease in ILSS values while going from thin to thick laminates because of the internal resistance offered by thick laminates. Also, ILSS values were improved when CNT reinforcement was increased. Ozkan Ozbek used double and triple hybrid combinations of S-glass, Carbon and Kevlar composites for failure analysis [8]. Ply delamination, fiber crushing, kink band formation, etc, these types of composite failures were observed during ILSS testing. While hybridization fiber type, position and stacking sequence plays an important role in improving ILSS. Srikanth Goruganthu examined the effects of field exposure and extreme conditions on ILSS of carbon/epoxy composites [9]. Enhancement in ILSS was observed under hot conditions due to improved crosslink density. T. Scalici used Hand-impregnated vacuum bagging and Vacuum assisted resin infusion manufacturing processes to fabricate basalt/epoxy composites and then ILSS, DCB and ENF tests were performed on them [10]. It was found that the hand-layup technique followed by vacuum bagging produced a better impregnation of the laminate. V. Balasubramani performed ILSS and flexural modulus testing by varying laminate thickness, resin type and stacking sequence [11]. Analytical and experimental values were compared and a slight error was found in ILSS values and a higher percentage error was found in flexural modulus values. P. Feraboli performed a four-point bend ILSS test on uni-directional and multi-directional carbon/epoxy composites [12]. And the results were validated using ANSYS software. A. A. Pradhan obtained the performance characteristics of Basalt-Carbon mixed fiber laminates by finite element analysis [13]. It was established that by placing a basalt layer in the core part and carbon layers in the outer parts, the strength of the composite laminate improved.

C. Nightingale examined two epoxy systems selected based on their dielectric loss factors and toughened with polyetherimide (PEI) [14]. Unidirectional carbon fiber prepreps were prepared and cured using three methods: autoclave, partial autoclave with microwave post-curing, and full microwave curing. It was found that microwave curing led to higher void content due to lower pressure, impacting mechanical properties. Zhihang Fan analysed the enhancement of interlaminar shear strength (ILSS) of GFRP composites using infusion of multi-walled carbon nanotube (MWNT)-epoxy suspension into glass fiber mats [15]. Short beam shear (SBS) and compression shear tests (CST) were conducted, CST providing more consistent ILSS values. Dilip Kumar investigated the influence of ply sequence on ILSS symmetric and asymmetric GFRP laminates [16]. Yihong, He presented an FE simulation to characterize nonlinear shear stress-strain behaviour and ILSS of unidirectional polymeric laminates by the short beam shear (SBS) test [17]. Computations indicated that increased loading nose diameters minimized the stress concentration but had little influence on shear stress distribution. Shreya Singh examined the effect of stacking sequence and thermal conditioning (27°C, 50°C, and 80°C) on flexural and interlaminar shear strength (ILSS) of basalt/flax hybrid fiber composites produced using an autoclave [18]. Results indicated that basalt-laminates over flax-laminates were better because basalt fibers are much (2.28 times) stronger compared to flax. Prashant Rawat investigated the improvement of ILSS by varying percentages of MWCNT content, where laminates were prepared by hand lay-up and vacuum bagging techniques [19].

The experiment revealed that the best improvement was achieved when the laminate was laminated with 0.5 wt.% MWCNT.

GFRP and CFRP composites have been studied extensively in the recent years. But there has been limited research on Basalt-reinforced composites. Hence, the objective of this research is to find out the Interlaminar Shear Strength of Basalt Fiber Reinforced Polymer. And validating the experimental results using simulation software ANSYS. This study also investigated failure mechanisms including delamination, matrix cracking, fiber-matrix debonding, and related phenomena.

## Experimental Procedure

### Material Fabrication

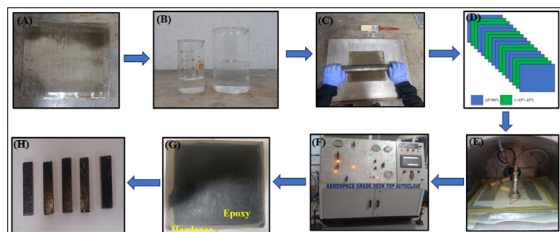
BFRP bi-directional laminate plates were fabricated using 16 layers of plain weave fabrics made from basalt with an areal density of 380 GSM. The basalt fabric sheet was provided by the Chennai based vendor 'Fiber Region'. The material properties of basalt fiber are outlined in Table 1(A). Each layer was approximately 0.3 mm thick so the total thickness of the laminate was around 6 mm which was according to the ASTM D2344 standard. Fabrication was done by hand layup technique followed by Autoclave curing. To fabricate the laminated plates, firstly, laminae sheets were cut into the required size (Figure 1A). Before the hand layup process, a mold release agent and wax were applied on the flat surface to ensure the easy removal of laminate. Then epoxy resin (LY556) and hardener (HY951) were amalgamated in the weighted ratio of 10:1 (Figure 1B), and the mixture was then placed in the furnace at a temperature around 500C for 20 min to release all the bubbles and flatten the mixture. Epoxy was taken in the ratio of 50:50 with respect to fiber weight. After applying epoxy and placing the first layer of fiber sheet, the steel roller was rolled over the layer to remove the entrapped air and excess epoxy (Figure 1C). The laminates were stacked in the sequence [(0/90), (45/-45), (45/-45), (0/90)]<sub>2s</sub> (Figure 1D). After completing the hand layup process, a perforated sheet and bleeder cloth were placed over the layup which is used to conduct the vacuum path into the laminate. Then the sealant tape is applied around the boundary of the layup, and the vacuum bag is placed above the sealant and was sealed properly (Figure 1E). Then the entire setup was carefully placed inside the autoclave chamber for curing process (Figure 1F). After curing, it is kept in the chamber for about 8 hr. The cured laminates were then cut into the required size using a diamond cutter (Figure 1H). The free edges of the laminates were smoothened with the help of sand paper to lower the possibility of edge-related damage during testing.

**Table 1(A): Material properties of Basalt fabric**

Property	Value	Unit	Tolerance
Density	2.63	Kg/m <sup>3</sup>	+/-5%
Surface density	380	g/m <sup>2</sup>	+/-5%
Melting Point	1350	C°	+/-100
Weave type	Plain		
Weft and warp Yarn specification	13micro 345tex		
Weft and warp picks	6X5 (ends/10mm)		+/-0.5
Sizing type	Silane		

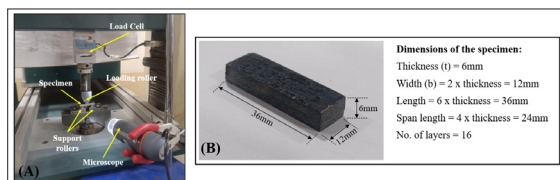
**Table 1(B): Physical properties of epoxy and hardener [5]**

Property	Epoxy (LY556)	Hardener (HY951)
Appearance	Medium viscous	Clear liquid
Viscosity	9-12 GPa	0.5-1 GPa
Density	1.13-1.16g/cc3	0.843g/cc3
Mixing ratio	10	1

**Figure 1:** Fabrication process of BFRP laminate

### Experimental Setup

The Hounsfield H50KS is a computerized Universal Testing Machine (UTM) having capacity of 50 KN was used to determine the ILSS. The system is located at SOM lab, IIT (ISM), Dhanbad, India. The setup for the test is shown in Figure 2A and Figure 2B shows the sample dimensions according to the standards. Five sample specimens were tested for the ILSS test in compliance with the American Society for Testing and Materials (ASTM) standards. This standard test is issued under the ASTM D2344 standards with Short Beam Shear (SBS) specimen [14]. The flexural strengths and loads were measured and the average values were reported.

**Figure 2:** Experimental Setup and dimensions of the SBS test specimen

Interlaminar Shear Strength (ILSS) of the composite is evaluated by the following equation,

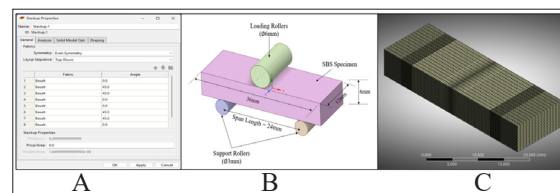
$$ILSS = \frac{3P_m}{4bt} \quad (1)$$

Where,  $P_m$  is the maximum load applied in  $N$ .

### Numerical Study

For investigation of ILSS the finite element analysis software ANSYS 24R2 was used to perform numerical stress analyses. The mechanical properties of the basalt fiber were taken from the literature review as shown in Figure 4. For loading and support rollers, structural steel was assigned as a material. The specimen was then modelled in ANSYS Composite PrePost (ACP) by taking the required dimensions. The stack-up properties of 16 layered composite are shown in Figure 3(A). The thickness of each layer was taken as 0.375 mm. Meshing was performed on the generated laminate as shown in Figure 3(C). Fine meshing

was generated near the loading and support rollers to achieve more accurate results and coarse meshing was generated away from the rollers to reduce the computational time. Frictional contact of friction coefficient 0.1 was provided between the loading roller and laminate whereas the contact between support rollers and laminate was frictionless. For all the contacts, 'Adjust to touch' was given as an interface treatment and a pinball radius of 2 mm was provided. The 'Adjust to Touch' feature in ANSYS is used to eliminate any gaps or overlaps between contacting surfaces in your model, ensuring that they start in proper contact from the beginning of the analysis. The downward velocity of 1 mm/min was given to the loading roller as per the ASTM standards and support rollers were completely fixed.

**Figure 3(A):** Stack-up properties defined in ACP**Figure 3(B):** ILSS test setup in ANSYS**Figure 3(C):** Meshing

For investigation of ILSS the finite element analysis software ANSYS 24R2 was used to perform numerical stress analyses. The mechanical properties of the basalt fiber were taken from the literature review as shown in Figure 4. For loading and support rollers, structural steel was assigned as a material. The specimen was then modelled in ANSYS Composite PrePost (ACP) by taking the required dimensions. The stack-up properties of 16 layered composite are shown in Figure 3(A). The thickness of each layer was taken as 0.375 mm. Meshing was performed on the generated laminate as shown in Figure 3(C). Fine meshing was generated near the loading and support rollers to achieve more accurate results and coarse meshing was generated away from the rollers to reduce the computational time. Frictional contact of friction coefficient 0.1 was provided between the loading roller and laminate whereas the contact between support rollers and laminate was frictionless. For all the contacts, 'Adjust to touch' was given as an interface treatment and a pinball radius of 2 mm was provided. The 'Adjust to Touch' feature in ANSYS is used to eliminate any gaps or overlaps between contacting surfaces in your model, ensuring that they start in proper contact from the beginning of the analysis. The downward velocity of 1 mm/min was given to the loading roller as per the ASTM standards and support rollers were completely fixed.

Properties of Outline New 3: Basalt Fiber					
Property	Value	Unit			
1 Material Field Variables	Table				
2 Density	1830	kg m <sup>-3</sup>			
3 Orthotropic Elasticity					
4 Young's Modulus X direction	38900	MPa			
5 Young's Modulus Y direction	7470	MPa			
6 Young's Modulus Z direction	7470	MPa			
7 Poisson's Ratio XY	0.281				
8 Poisson's Ratio YZ	0.455				
9 Poisson's Ratio XZ	0.281				
10 Shear Modulus XY	2710	MPa			
11 Shear Modulus YZ	2540	MPa			
12 Shear Modulus XZ	2710	MPa			
13 Bilinear Isotropic Hardening					
14 Tangent Modulus Type	Plastic				
15 Yield Strength	300	MPa			
16 Tangent Modulus	3300	MPa			
17 Orthotropic Stress Limits					
18 Tensile X direction	1220	MPa			
19 Tensile Y direction	62.1	MPa			
20 Tensile Z direction	62.1	MPa			
21 Compressive X direction	-780	MPa			
22 Compressive Y direction	-93.1	MPa			
23 Compressive Z direction	-93.1	MPa			
24 Shear XY	65.7	MPa			
25 Shear YZ	51.42	MPa			
26 Shear XZ	65.7	MPa			
27 Tensile Constants					
28 Coupling Coefficient XY	1				
29 Coupling Coefficient YZ	1				
30 Coupling Coefficient XZ	1				
31 Ply Type					
32 Type	Woven				

**Figure 4:** Mechanical properties of the Basalt Fiber [13]



## Result and Discussions

### Determination of ILSS

Five samples of Interlaminar Shear Strength test were analysed to ensure the accuracy of the results. Dimensions of all the five specimens were taken using a digital vernier caliper and were recorded as shown in Table 2. It also shows maximum flexural strength and maximum load recorded during the testing. The ILSS results of all the samples were calculated using equation

(1). Figure 5(A) shows the graph between the load applied and the displacement of the sample. And flexural strength versus strain curves are shown in Figure 5(B). Values for load and flexural strength were raised until they reached a point where cracks initiated, then they were lowered. The results indicate that the specimens exhibited similar behaviour with only slight differences, demonstrating high repeatability and dependable testing outcomes.

**Table 2: ILSS Test result**

Specimen No.	Thickness (mm)	Width (mm)	Length (mm)	Max. flexural strength (MPa)	Max. load (N)	ILSS (MPa)
1	5.65	11.96	36.62	565	2850	31.632
2	5.84	11.85	37.10	620	2910	31.537
3	5.67	11.50	37.25	577	2830	32.551
4	5.74	12.40	36.23	594	2880	30.347
5	5.64	11.70	38.22	598	2820	32.051
<b>Average</b>	<b>5.708</b>	<b>11.882</b>	<b>37.084</b>	<b>590.8</b>	<b>2858</b>	<b>31.624</b>

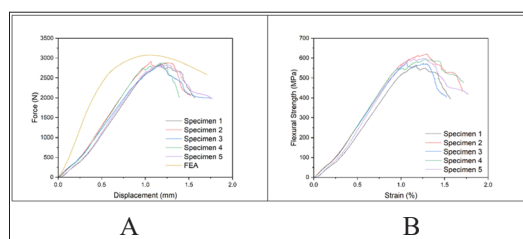


**Figure 5(A):** Experimental Force V/s Displacement graph of 5 specimens

**Figure 5(B):** Experimental Flexural Strength V/s Strain graph of 5 specimens

### Finite Element Analysis

FE Analysis was done in static structural after the composite modelling in ACP. The maximum load obtained during analysis was 3076.5 N, which is shown in Figure 7. Therefore, numerically, the ILSS value of BFRP is 32.046 MPa. Figure 6A shows the von-mises stresses, which also represent flexural strength. A maximum value of 599.88 MPa of strength was obtained during simulation. This value deviates from the experimental value by 1.33%. Figure 6B represents the shear stress, which is maximum in the lateral direction. Total deformation of the laminate is shown in Figure 6C. A maximum value of 1.708 mm was obtained at the centre of the specimen. The Composite Failure Tool was used to identify the crack formation. The Tsai-Wu failure criterion was kept ON, which predicts the composite failure by considering the total strain energy of a material. In Figure 6D red coloured section represents Inverse Reverse Factor (IRF) more than 1. The part is considered to be failed when  $IRF > 1$ . Matrix cracking is visible at the edge of the red coloured section.

### Damage Analysis

Celestron digital microscope (China) of 5MP (20-200x) was used to monitor the damage morphology in the ILSS test. Figure 7 shows the typical failure mechanisms like delamination, crack initiation, severe matrix cracking, fiber breakage, etc. which were observed during the ILSS test. The first stage of failure is crack initiation, which occurs because of stress concentration.

Due of continuous loading, it may result in a sudden breakdown of the specimen whose recovery is not possible. Delamination occurs because of the weak bonding between adjacent layers. Matrix cracking usually occurs due to voids or defects, it weakens the load bearing ability of the composite. When fibers exceed their ultimate tensile strength, they break, which leads to a sudden drop in load carrying capacity. Figure 8 shows the surface damage of the laminates. Because of the contact between the roller and laminate, surface damage occurs.

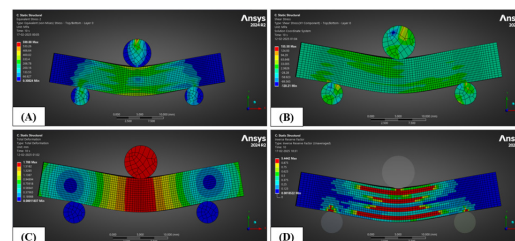


**Figure 6: Simulation Results**

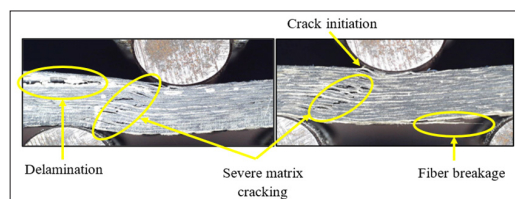


**Figure 7: Macroscopic images of damaged specimen**

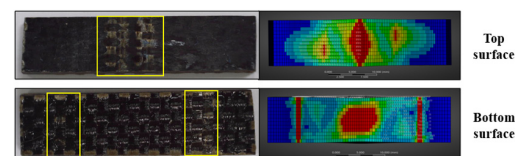


**Figure 8: Surface damage of the specimen**

### Conclusion

From the above results following points can be concluded:

1. From published literature [1], the ILSS of neat CFRP at 1 mm/min strain rate is 27.45 MPa, which is less than that of neat BFRP which has an ILSS value of 31.624 MPa.

2. The average maximum load by experimental and finite element analysis are 2858N and 3076.5N respectively. Therefore, the ILSS value by FEA is 32.046 MPa, which deviates from the experimental value by 1.33%.
3. Delamination, matrix cracking, crack initiation, fiber breakage, etc. these types of failure mechanisms were observed while performing experiments.
4. Composite failure tool in ANSYS Mechanical plots the ultimate strength with respect to von-mises stress with the help of Inverse Reverse Factor (IRF) at each node. Hence, the part is considered to be failed when the IRF value is more than 1.
5. Finite element analysis is a reliable method for simulating the fracture behaviour of composite materials based on their mechanical properties.

## References

1. Kumar S, Sharma N, Biswas R, Singh KK. Effect of temperature on the flexural and ILSS behaviour of symmetric and asymmetric basalt fibre-reinforced polymer composites. *Materials Today: Proceedings*. 2023.
2. Huang WJ, Li YT, Zhang YM, Xiao ZM, Li WG. Experimental and numerical investigations of interlaminar shear behaviors of CFRP composites at cryogenic and high temperatures. *Composite Structures*. 2025. 352: 118681.
3. Lakshmi PR, Devi PA, Reddy PR, Yamuna K, Bharathi Y. Estimation of interlaminar shear strength in glass epoxy composites by experimental and finite element method. In *Journal of Physics: Conference Series*. 2019. 1240: 012027.
4. Kumar C, Singh KK, Rawat P, Deep A, Behera RP. Effect of loading rate on inter laminar shear strength (ILSS) of highly doped MWCNTs carbon/epoxy laminates. In *IOP Conference Series: Materials Science and Engineering*. 2018. 455: 012006.
5. Sharma N, Singh KK. Transverse fatigue behavior analysis of symmetric and asymmetric glass fiber-reinforced laminates. *Polymer Composites*. 2023. 44: 2871-2886.
6. Zhang A, Lu H, Zhang D. Research on the mechanical properties prediction of carbon/epoxy composite laminates with different void contents. *Polymer Composites*. 2016. 37: 14-20.
7. Lakshmi PR, Akhil K. Estimation of ILSS in Neat Resin and CNT Reinforced S Glass Composites by Finite Element Analysis. *Journal of Materials Science and Engineering A*. 2019. 9: 143-148.
8. Özbek Ö, Bulut M, Erklığ A, Bozkurt ÖY. Interlaminar shear strength and failure analysis of composite laminates with double and triple hybrid configurations. *Engineering Structures*. 2022. 265: 114498.
9. Goruganthu S, Elwell J, Ramasetty A, Nair AR, Roy S, et al. Characterization and modeling of the effect of environmental degradation on interlaminar shear strength of carbon/epoxy composites. *Polymers and Polymer Composites*. 2008. 16: 165-179.
10. Scalici T, Pitarresi G, Badagliacco D, Fiore V, Valenza A. Mechanical properties of basalt fiber reinforced composites manufactured with different vacuum assisted impregnation techniques. *Composites Part B: Engineering*. 2016. 104: 35-43.
11. Balasubramani V, Nagarajan KJ. Experimental and optimization of interlaminar shear strength and flexural modulus of laminated composite materials under flexural loading. *Materials Today: Proceedings*. 2023.
12. Feraboli P, Kedward KT. Four-point bend interlaminar shear testing of uni-and multi-directional carbon/epoxy composite systems. *Composites Part A: Applied Science and Manufacturing*. 2003. 34: 1265-1271.
13. Shaikh AA, Pradhan AA, Kotasthane AM, Patil SS, Karuppanan S. Finite Element Analysis of Mechanical Properties of Basalt-Carbon Epoxy Hybrid Laminates. *Mechanics Of Advanced Composite Structures*. 2022. 9: 263-274.
14. Test Method for Short-Beam Strength of Polymer Matrix Composite Materials and Their Laminates, ASTM International, West Conshohocken, PA. 2022.
15. Nightingale C, Day RJ. Flexural and interlaminar shear strength properties of carbon fibre/epoxy composites cured thermally and with microwave radiation. *Composites Part A: Applied Science and Manufacturing*. 2002. 33: 1021-1030.
16. Fan Z, Santare MH, Advani SG. Interlaminar shear strength of glass fiber reinforced epoxy composites enhanced with multi-walled carbon nanotubes. *Composites Part A: Applied science and manufacturing*. 2008. 39: 540-554.
17. Kumar D, Singh KK, Ansari MTA. Effect of ply lay-up sequence on interlaminar shear strength of symmetric and asymmetric GFRP composite. *Materials Today: Proceedings*. 2020. 22: 2241-2246.
18. He Y, Makeev A. Nonlinear shear behavior and interlaminar shear strength of unidirectional polymer matrix composites: A numerical study. *International Journal of Solids and Structures*. 2014. 51: 1263-1273.
19. Singh S, Singh KK, Sharma N. Effect of stacking sequence and the temperature on the flexural and inter laminar shear strength behaviour of symmetric and asymmetric basalt/flax hybrid fibre reinforced composites. In *AIP Conference Proceedings*. 2024. 3178.
20. Rawat P, Singh KK. A strategy for enhancing shear strength and bending strength of FRP laminate using MWCNTs. In *IOP Conference Series: Materials Science and Engineering*. 2016. 149: 012105.
21. Liu Y, Yang JP, Xiao HM, Qu CB, Feng QP, et al. Role of matrix modification on interlaminar shear strength of glass fibre/epoxy composites. *Composites Part B: Engineering*. 2012. 43: 95-98.
22. Abali F, Pora A, Shivakumar K. Modified short beam shear test for measurement of interlaminar shear strength of composites. *Journal of composite materials*. 2003. 37: 453-464.